North Atlantic Oscillation controls on oxygen and hydrogen isotope gradients in winter precipitation across Europe; implications for palaeoclimate studies

5 Michael Deininger[1], Martin Werner[2], Frank McDermott[1,3]

[1]UCD School of Earth Sciences, University College Dublin, Belfield, Dublin 4, Ireland
[2]Alfred Wegener Institute, Helmholtz Centre for Polar and Marine Research, Bussestraße 24, 27570 Bremerhaven, Germany
[3]UCD Earth Institute, University College Dublin, Belfield, Dublin 4, Ireland

10 *Correspondence to*: Michael Deininger (michael.deininger@ucd.ie)

Abstract. Winter (October to March) precipitation $\delta^{18}O_P$ and δD_P values in central Europe correlate with the winter NAO index (wNAOi), but the causal mechanisms remain poorly understood. Here we analyse the relationships between precipitation-weighted $\delta^{18}O_P$ and δD_P datasets ($\delta^{18}O_{pw}$ and δD_{pw}) from European GNIP and ANIP stations and the wNAOi, with a focus on isotope gradients. We demonstrate that longitudinal $\delta^{18}O_{pw}$ and δD_{pw} gradients across Europe (continental

15 effect) depend on the wNAOi state, with steeper gradients associated with more negative wNAOi states. Changing gradients reflect a combination of air temperature and variable amounts of precipitable water as a function of the wNAOi. The relationships between the wNAOi, $\delta^{18}O_{pw}$ and δD_{pw} can provide additional information from palaeoclimate archives such as European speleothems that primarily record winter $\delta^{18}O_{pw}$. Comparisons between present-day and past European longitudinal $\delta^{18}O$ gradients inferred from Holocene speleothems suggest that atmospheric pressure configurations akin to

20 negative wNAO modes dominated the early Holocene, whereas patterns resembling positive wNAO modes were more common in the late Holocene, possibly caused by persistent shifts of the relative locations of the Azores High and the Icelandic Low.

1 Introduction

Stable oxygen and hydrogen isotopes ($\delta^{18}O$, δD; relative to Vienna Standard Mean Ocean Water) in precipitation have been

25 analysed extensively since the 1950s (Dansgaard, 1954;Craig, 1961;Craig and Gordon, 1965) to decipher environmental processes that control their variations and to facilitate their use in palaeoclimatology (Dansgaard, 1964;Gat, 1996;Rozanski et al., 1992;Aggarwal et al., 2012). The Global Network of Isotopes in Precipitation (GNIP) program initiated in 1958 by the International Atomic Energy Agency (IAEA) and the World Meteorological Organization (WMO) has operated since 1961, and has made great progress towards these aims (e.g. Dansgaard, 1964;Rozanski et al., 1992). For the European sector of the

30 GNIP program, 438 stations have operated, with the oldest records from the GNIP stations at Valentia Observatory in Ireland (since 1958), and at Hohe Warte (Vienna, Austria) since 1960. The processes that drive $\delta^{18}O$ values in precipitation ($\delta^{18}O_P$)

at these stations have been discussed extensively in the literature, focusing mainly on air temperature, altitude and the continental effect (Rozanski et al., 1982;Stumpp et al., 2014;Schürch et al., 2003;Lykoudis and Argiriou, 2011;Fischer and Baldini, 2011). In recent years, several studies have investigated the relationship between the North Atlantic Oscillation (NAO) – the major atmospheric mode of European winter climate, (Hurrell et al., 2003;Hurrell and VanLoon, 1997;Hurrell, 1995) – and $\delta^{18}O_P$ at specific stations (Baldini et al., 2008;Langebroek et al., 2011;Field, 2010). More recently, the effect of the East Atlantic pattern, the second major mode of atmospheric pressure variability in the North Atlantic region (Barnston and Livezey, 1987) on the relationship between the winter NAO index (wNAOi) and the $\delta^{18}O_P$ in Europe has been examined (Comas-Bru et al., 2016). A complementary approach, developed here, is to document and seek to understand the *longitudinal gradients* in winter rainfall $\delta^{18}O_P$ across Europe, and to link these to different states of the NAO.

Here we present a detailed station-based evaluation of the effects of the wNAOi on precipitation-weighted $\delta^{18}O_P$ and δD_P values ($\delta^{18}O_{pw}$ and δD_{pw}) during the winter season for continental Europe and the Alps. We demonstrate that the well-documented longitudinal gradient in $\delta^{18}O_{pw}$ and δD_{pw} across the European continent (often referred to as the 'continental effect') depends on the state of the winter NAO index (wNAOi), through a combination of air temperature and atmospheric precipitation history effects. The downstream effects of this wNAOi–linked variability can also be detected in the $\delta^{18}O_{pw}$ and δD_{pw} values at stations north of the Alpine divide. We also make use of the $\delta^{18}O_{pw}$ and δD_{pw} outputs from an isotope-enabled General Circulation Model ECHAM5-wiso (Werner et al., 2011;Langebroek et al., 2011) to better evaluate the NAO-dependence of the longitudinal isotope gradients. This study improves our understanding of the significance of inferred past changes in $\delta^{18}O_{pw}$ or δD_{pw} gradients across Europe, for example during the course of the Holocene (e.g. McDermott et al., 2011) by linking modern $\delta^{18}O_{pw}$ and δD_{pw} gradients, respectively, to different states of the wNAO and/or changes in the European continental temperature gradient and atmospheric precipitation histories.

2 Data and Methods

2.1 Station-based data

Monthly winter (October to March) $\delta^{18}O_P$ and δD_P, temperature and precipitation data from 37 European stations were used to investigate the dependence of $\delta^{18}O_{pw}$ and δD_{pw} values on the wNAOi (Figure 1).

Thirty-one of these stations are part of the GNIP network and six are part of the Austrian Network of Isotopes in Precipitation (ANIP). The data from the ANIP stations originate from Humer (1995) and the ANIP homepage (http://wisa.bmlfuw.gv.at/daten.html). The GNIP stations were selected based on recent findings, showing that the un-weighted winter (December to March) $\delta^{18}O_P$ and δD_P values at these stations are significantly correlated with the wNAOi (Baldini et al., 2008). The ANIP stations were selected for their long records starting in the early 1970s and their location, which ensures that there are sufficient $\delta^{18}O_P$ and δD_P measurements in the Alps for the purposes of this study. For our

analysis, the wNAOi is the average winter value calculated from the monthly PC-based NAOi values from December to
March (Hurrell, 1995) downloaded from the Climate Data Guide[1]. For every station, the $\delta^{18}O_{pw}$ and δD_{pw} values were
calculated for each winter, using the monthly $\delta^{18}O_P$ and δD_P values, weighted by the monthly precipitation amounts, for the
period October to March (6 month) and December to February (3 month). The studied periods are chosen on the one hand
because during December to February the NAO exerts its strongest influence on the European winter climate (e.g. Hurrell,
1995) and we expect to observe the strongest influence on $\delta^{18}O_P$ and δD_P in this 3-month period and on the other hand
because the main infiltration period for precipitation in central Europe is from October to March and is, therefore, the period
of interest for palaeoclimate archives recording the infiltrated $\delta^{18}O_{pw}$ and δD_{pw} in this 6-month interval (e.g. speleothems).
For further analysis, the winter $\delta^{18}O_{pw}$ and δD_{pw} values (6 month and 3 month) of every station are grouped into six classes
depending on the wNAOi. The wNAOi was sub-divided into six classes (bins): (i) $1.6 \leq$ wNAOi; (ii) $0.8 \leq$ wNAOi < 1.6;
(iii) $0 \leq$ wNAOi < 0.8; (iv) $-0.8 \leq$ wNAOi < 0; (v) $-1.6 \leq$ wNAOi < -0.8; (vi) wNAOi < -1.6, resulting in six compilations of
$\delta^{18}O_{pw}$ and δD_{pw} values for every station. For every station, the median of every compilation was calculated. An example is
given in Figure 2, which shows how the data were processed, resulting in six median $\delta^{18}O_{pw}$ and δD_{pw} values for the
Garmisch-Partenkirchen station (#24 in Figure 1).

For the analysis of the processed $\delta^{18}O_{pw}$ and δD_{pw} values, the stations were also subdivided into continental stations, which
includes all stations with an altitude ≤ 350m and having no (or negligible) Mediterranean influence (distance to the
Mediterranean coastline > 100 km) (13 stations); and stations with an altitude >350m. The latter stations were divided into
two groups: continental stations with an altitude higher than 350m (3 stations) and Alpine stations (17 stations).
Furthermore, four Mediterranean GNIP stations south of the Alps were analysed to better validate the $\delta^{18}O_{pw}$ and δD_{pw}
values of the Alpine regions (Figure 1).

3 Results

3.1 Results of the longitudinal $\delta^{18}O_{pw}$ and δD_{pw} gradients (continental stations)

To study the relationship between the wNAOi classes and the longitudinal $\delta^{18}O_{pw}$ and δD_{pw} gradients during the winter
season, $\delta^{18}O_{pw}$, δD_{pw} datasets of a total of 13 'continental' GNIP stations are analysed. (This includes the two maritime sites
Valentia Observatory; Ireland, (station #1) and Wallingford, England, (station #2).) The most westerly station is at -10.25 °E
(Valentia Observatory; Ireland) and the easternmost station is at 19.85 °E (Krakow, Poland) (Figure 1). These continental
stations show a positive sensitivity of $\delta^{18}O_{pw}$ and δD_{pw} to the wNAOi (Figure 3), i.e., a positive linear relationship with the
wNAOi for the investigated continental station datasets, resulting in more positive median $\delta^{18}O_{pw}$ and δD_{pw} values for higher

---

[1] The Climate Data Guide: Principal Component based North Atlantic Oscillation (NAO) Index:
https://climatedataguide.ucar.edu/climate-data/hurrell-north-atlantic-oscillation-nao-index-pc-based.

wNAOi classes, as in Figure 2 for Garmisch-Partenkirchen. An exception to this observation is the GNIP stations Valentia Observatory (Station 1) where the $\delta^{18}O_{pw}$ and δD_{pw} values do not show a clear linear relationship compared to the other continental stations for either the 3-month (Figure 3a and 3c) or 6-month (Figure 3b and 3d) winter periods. Similar behaviour is seen in the data for the Wallingford GNIP station (Station 2) for the 6-month winter period (Figure 3b and 3d). This behaviour is likely to be caused by the proximity of these two maritime stations to the North Atlantic. It is notable, that for most stations, the sensitivity of $\delta^{18}O_{pw}$ and δD_{pw} to the wNAOi is higher for the 3-month winter period than for the 6-month winter period (Figure 3). The median sensitivity for $\delta^{18}O_{pw}$ is 0.87 (3 month) and 0.57 (6 month) ‰/wNAOi unit, and for δD_{pw} 6.87 (3 month) and 4.44 (6 month) ‰/wNAOi unit. This likely reflects the fact that the mode of the wNAOi (December to March) exerts the strongest influence on European winter meteorology (e.g. Hurrell, 1995;Hurrell et al., 2003), and so on $\delta^{18}O_{pw}$ and δD_{pw} (see discussion in Section 4.1).

To investigate the dependence of the longitudinal $\delta^{18}O_{pw}$ and δD_{pw} gradients from these 13 continental stations on the wNAOi classes, the gradient slopes were calculated for each of the six wNAOi classes. For all winter month periods the slope is negative (towards the east) indicating that the $\delta^{18}O_{pw}$ and δD_{pw} values become more negative towards the east. Furthermore, the slopes of the longitudinal $\delta^{18}O_{pw}$ and δD_{pw} gradients of the continental stations becomes steeper for winters with more negative wNAOi classes (Figure 4). This means that ^{18}O and ^{2}H are more efficiently removed from the atmospheric moisture with distance from the western margin, resulting in more strongly negative $\delta^{18}O_{pw}$ and δD_{pw} values along the longitudinal transect during more negative NAO winters compared with more positive NAO winters. Furthermore, the slope is steeper for the 3-month (DJF) averages compared with that for the 6-winter month averages.

Comparison of the longitudinal $\delta^{18}O_{pw}$ and δD_{pw} gradients derived from ECHAM5-wiso simulations with those from the station-based data show that slopes from the ECHAM5-wiso data reproduce the observed station-based slopes quite well (Figure 4). Only the slopes determined for the most negative wNAOi class of the 6-month winter period level off from the empirically determined slopes (Figure 4a and 4c). Overall, however, there is good agreement between the ECHAM5-wiso isotope gradients and those derived from the observational datasets (see supplementary material for a detailed discussion on ECHAM5-wiso simulations).

3.2 Alpine stations and other stations with an altitude > 350m

Data from European stations with an altitude greater than 350m are separated into two groups: Alpine stations and non-Alpine stations. The non-Alpine stations include Wasserkuppe-Rhoen (#20, 921m), Hof-Hohensaas (#28, 567m) and Regensburg (#29, 377m), all located in Germany (Figure 1). These show similar $\delta^{18}O_{pw}$ and δD_{pw} sensitivity to the wNAOi as the other continental stations (Figure 3). The Alpine stations include a total of 17 stations that are well distributed over the Alps (Figure 1). These data allow an evaluation of precipitation $\delta^{18}O_{pw}$ and δD_{pw} values and patterns in the entire Alpine region as a function of the wNAOi. The sensitivity analysis of $\delta^{18}O_{pw}$ and δD_{pw} of the Alpine stations reveals a somewhat

more complex relationship to the wNAOi. For the 3-month winter period, the $\delta^{18}O_{pw}$ data from the Thonon-Les-Bains (14), Längenfeld (21), Obergurgl (23), Böckstein (30), St. Peter (31), Villacher Alpe (32), Graz University stations (33) have a weak or absent relationship to the wNAOi, while the $\delta^{18}O_{pw}$ and δD_{pw} data from the other Alpine stations have a similar sensitivity to the wNAOi as the continental stations (Figure 3a). The δD_{pw} data show similar results as $\delta^{18}O_{pw}$, but there are

130   different results for some other stations. For Thonon-Les-Bains (14) the relationship between δD_{pw} and the wNAOi is stronger compared to $\delta^{18}O_{pw}$ whereas the relationship for Grimsel is weaker (18) (Figure 3c). For the 6-month winter period, the $\delta^{18}O_{pw}$ sensitivity to the wNAOi for most of the Alpine stations is comparably strong to that of the continental stations. Only the stations at Thonon-Les-Bains (14), Längenfeld (21), Böckstein (30), St. Peter (31), Villacher Alpe (32), Graz University (33) show a weak relationship to the wNAOi (like for the 3-month winter period). The Obergurgl station (23) has

135   a stronger relationship to the wNAOi compared with the 3-month winter period but has a smaller average $\delta^{18}O_{pw}$ sensitivity compared with the other Alpine stations. The highest $\delta^{18}O_{pw}$ sensitivity can be found for Hohenpeißenberg (22) and Regensburg (29) and is 0.77 ‰/wNAOi unit (Figure 3b). The δD_{pw} sensitivity of the Alpine stations for the 6-month winter period shows a similar relationship as for the 3-month winter period. For stations in Bern (15), Guttannen (17), Obergurgl (23) and Villacher Alpe (32), however, the conclusion is different compared with the 3-month winter period. The

140   relationship of δD_{pw} to the wNAOi is weaker for Bern (17) whereas it is stronger for the other stations. The highest sensitivity is observed for the Thonon-Les-Bains (14) and Meiringen (16) stations and is 7.42 and 8.84 ‰/wNAOi unit, respectively (Figure 3d).

4 Discussion

4.1 Longitudinal $\delta^{18}O_{pw}$ and δD_{pw} gradients

145   To explain the change in the slopes of the longitudinal winter $\delta^{18}O_{pw}$ and δD_{pw} gradients (Figure 4), the measured temperatures and the amount of precipitation at the GNIP stations are evaluated. The GNIP station based continental temperature and precipitation gradients for the different wNAOi classes show that the slopes of the longitudinal winter temperature gradients become steeper for lower wNAOi values and are always negative (i.e. average winter temperatures are always lower in the east), but no equivalent relationship is observed for the slopes of the winter precipitation gradients

150   (Figure 5). (The following conclusions are not hampered if the two maritime sites Valentia Observatory and Wallingford, station #1 and #2 (Figure 1), are omitted from the compilation of all 'continental stations' (Figure S1).) The temperature relationships suggests that while the winter air temperature clearly becomes colder from west to east, a higher average air temperature gradient between western and eastern Europe occurs in more negative wNAOi winters. Furthermore, the intercept of the linear regression is progressively smaller for more negative wNAOi modes, suggesting general cooler

155   conditions in central Europe during negative wNAOi modes. This is consistent with the general relationship between the wNAOi and winter air temperatures for central Europe (e.g. Hurrell, 1995;Comas-Bru and McDermott, 2013). Curiously, for the most negative wNAOi class, the slope of the temperature gradient does not follow the general trend and has a lower

value, comparable to more positive winter wNAOi modes, suggesting a smaller temperature difference between western and eastern Europe under these conditions. The reason for this change is unclear and reflects possibly a relationship of the cyclone variability to the NAO (Gulev et al., 2001), which may increase the frequency of incursions of cold easterly winds into western Europe during very negative wNAO modes.

The observed temperature slopes can be used to calculate the expected air temperature-driven difference in $\delta^{18}O_{pw}$ and δD_{pw} between the western- and eastern-most GNIP stations using theoretical temperature sensitivities for $\delta^{18}O_P$ and δD_P (e.g. from Dansgaard, 1964). The theoretical changes in $\delta^{18}O_{pw}$ and δD_{pw} between the western- and eastern-most GNIP stations (the longitudinal difference between the Valentia (Observatory) and Krakow (Wola Justowska) is 30.1°) were calculated as follows. First, the temperature difference between these two stations was calculated from the temperature slope for the different wNAOi classes. For example, for the highest wNAOi class, the slope of the observed temperature gradient is -0.19 K/°E and -0.26 K/°E for the 6-month and 3-month winter period, resulting in a temperature difference of 5.86 K and 7.78 K, respectively. Hence, the average winter temperature at Valentia Observatory from October to March (December to February) is about 5.86 K (7.78 K) warmer compared to Krakow Wola Justowska for the highest wNAO class. The effect of this eastward temperature decrease can be converted into an expected $\delta^{18}O_{pw}$ and δD_{pw} difference between the two stations. For this estimate we apply an approximate estimation of the sensitivity of $\delta^{18}O_P$ and δD_P on temperature changes based on theoretically derived values by Dansgaard (1964), assuming a Rayleigh-type moist adiabatic condensation (vapour-liquid) process. For the sensitivity, the average value for a cooling from an initial temperature of 0°C to -20°C is used, which is 0.64 ‰/K for $\delta^{18}O_P$ and 5.6 ‰/K for δD_P (Dansgaard, 1964). Hence, for the highest wNAO class, the observed temperature difference would cause a calculated difference of 3.75 ‰ (6-month) and 4.98 ‰ (3-month) for $\delta^{18}O_{pw}$. $\delta^{18}O_{pw}$ values are therefore expected to be 3.75 ‰ and 4.98 ‰ lighter at the easternmost station compared to the westernmost station for the 3 winter month and 6 winter month averages, respectively.

These theoretical calculated values are now compared with the observed differences derived from the slopes of the linear regression of the GNIP $\delta^{18}O_{pw}$ datasets (Figure 4). For the highest wNAO class, the slope is -0.16 ‰/°E and 0.20 ‰/°E for the 6-month and 3-month winter period. This results in an observed difference of 4.78 ‰ (6-month) and 6.02 ‰ (3-month). Importantly, the observed differences (longitudinal gradients) are much larger than those calculated using the air-temperature driven Dansgaard-type model described above. The results of these calculations for $\delta^{18}O_{pw}$ and δD_{pw}, based on the observed temperature slopes, and for all wNAO classes are listed in Table 1.

The most important result of this simple exercise is that the observed differences in $\delta^{18}O_{pw}$ and δD_{pw} between the western- and eastern-most GNIP stations are larger than can be accounted for by a simple air temperature driven Rayleigh distillation model alone (Table 1). Repeating the calculations using the sensitivity of $\delta^{18}O_{pw}$ and δD_{pw} for the vapour-ice phase change (snow) (0.73 ‰/K for $\delta^{18}O_P$ and 6.2 ‰/K for δD_P, Dansgaard, 1964) instead results in calculated differences that are still too small to explain the observed differences in $\delta^{18}O_{pw}$ and δD_{pw} between the western- and eastern-most stations (not shown).

This strongly indicates that the observed longitudinal variations in winter air temperatures alone simply are insufficient to account for the observed difference between $\delta^{18}O_{pw}$ and δD_{pw} in western and eastern Europe, and that additional processes must be considered.

195

Rozanski et al. (1982) pointed out that the precipitation history of air masses is an important control on observed longitudinal δD_P gradients. Precipitation history can be expressed as a numerical value f (fraction of remaining moisture). Hence, f depends on the balance between the amount of precipitation (P) that has already occurred along the longitudinal gradient and the initial amount of precipitable water in the atmosphere (Q_0). However, only weak relationships are found between the

200   precipitation gradients calculated from the GNIP station precipitation datasets and the wNAOi classes, suggesting that rainfall gradients between western and eastern Europe are fairly constant, within the range of uncertainty (Figure 5c and 5d). Furthermore, the intercept of the linear regression of the precipitation data shows no dependence with the class of the wNAOi. This is consistent with the findings of Baldini et al. (2008) who showed that precipitation data from continental GNIP stations have no systematic correlation to the wNAOi (opposite to temperature). As discussed below, this points to

205   differences in the initial amounts of precipitable water (Q_0) as a possible control on isotope gradient-wNAOi relationships (Figure 4), over and above those attributable to air temperature gradients alone.

To better constrain the governing physical mechanisms of the precipitation history f and their first-order effects on $\delta^{18}O_{pw}$ and δD_{pw}, a simple one-box Rayleigh-type model for the atmosphere was used (Dansgaard, 1964;Eriksson, 1965):

210

$$^{x}R = {}^{x}R_0 \cdot f^{\,{}^{x}\alpha-1} = {}^{x}R_0 \left(\frac{Q}{Q_0}\right)^{{}^{x}\alpha-1} = {}^{x}R_0 \left(1 - \frac{P}{Q_0}\right)^{{}^{x}\alpha-1}. \tag{1}$$

Equation (1) is the classic Rayleigh distillation model (Rayleigh, 1902; see also Mook, 2006 for detail) that describes the evolution of an isotope ratio R (the subscript x is a place holder for x = 2 (^{2}H) or 18 (^{18}O), i.e., for $^{18}R=^{18}O/^{16}O$ and

215    $^{2}R=^{2}H/^{1}H$) as a function of the precipitation history f. This is a function of the amount of initial (Q_0) and remaining (Q) precipitable water in the atmosphere; Q is therefore the amount of precipitable water after a specific amount of precipitation P (Q_0-Q=P) has formed. R_0 describes the initial isotope ratio. α is the equilibrium liquid-water isotope fractionation factor that depends only on temperature; the subscript x denotes, as above, the related isotope system. Because the slope of the longitudinal precipitation gradient does not change systematically with the wNAOi class, P does not change with the class of

220   the wNAOi, and has, therefore, a negligible effect on $\delta^{18}O_{pw}$ and δD_{pw}. Hence, the slope of the longitudinal gradient of $\delta^{18}O_{pw}$ and δD_{pw} in central Europe is driven only by the temperature dependent isotope fractionation factor α, and by the initial amount of precipitable water Q_0 in the atmosphere. Although the classic Rayleigh-type model, adopted here is unable to fully capture all atmospheric processes (e.g. mixing of atmospheric moisture with different isotope signatures and/or origins), it is nonetheless a useful first approximation to explain the deviations between the calculated (temperature effect)

225 and observed differences in $\delta^{18}O_{pw}$ and δD_{pw} between the western- and eastern-most stations. Therefore, our observations of the dependence of the longitudinal $\delta^{18}O_{pw}$ and δD_{pw} gradient on the class of the wNAOi can be explained if additionally the amount of precipitable water over central Europe is lower for more negative wNAOi values. As demonstrated previously in a comparison of very positive (wNAOi>1) and negative (wNAOi<-1) wNAOi values, the maximum amount of precipitable water in the atmosphere is shifted southward for very negative wNAOi (Trigo et al., 2002). This shift in the amount of

230 precipitable water is associated with changing air temperature patterns, and smaller amounts of precipitable water are associated with cooler continental air temperatures. Accordingly, our simple model shows that the atmosphere in central Europe contains less (more) atmospheric moisture during more negative (positive) wNAOi states, and this is independently supported by analysis of the amount of precipitable water in the atmosphere from a NCEP/NCER reanalysis dataset (see below). Hence, atmospheric moisture $\delta^{18}O$ and δD values are likely to be more sensitive to the rainout history during more

235 negative wNAOi modes, because f must change at a higher rate if Q_0 is smaller and P is held constant (Eq. 1). This effect is also confirmed by a multi-box exercise that assumes a Rayleigh-type condensation process, mimicking the longitudinal gradients. This multi-box exercise shows that $\delta^{18}O_P$ becomes progressively depleted in dependence on Q_0 from west to east across Europe, with steeper gradients (higher slopes) for smaller Q_0 (Figure S2).

240 The wNAOi-precipitable water relationship described by Trigo et al. (2002) is also evident in the NCEP/NCER reanalysis dataset (and the ECHAM5-wiso simulations, see supplementary material) (Figure 6a). The NCEP/NCER reanalysis dataset covers the period from 1948-2016 and is analysed for the winter months December to March; it has a spatial resolution of 2.5°x2.5°. Precipitable water shows a positive correlation with wNAOi values in central and northern Europe (where all continental stations are located), and a negative correlation over the Mediterranean (including Iberia, the Balkans and

245 Turkey) (Figure 6). (Interestingly, the boundary between the area of positive and negative correlation lies within the Alpine region, though the coarse resolution does not allow any detailed conclusion for individual Alpine stations.) This indicates that during positive wNAO modes, the amount of precipitable water increases over central Europe and decreases during negative wNAO modes. This finding is also confirmed by the amount of precipitable water of the analysed NCEP/NCER reanalysis grid cells (Figure 6b and 6c). The results of the regression analysis of the longitudinal gradient of the precipitable

250 water shows that the slope of the precipitable water along the longitudinal gradient is rather independent (within the range of uncertainties, although a slight trend is visible indicating a shallower slope for more negative NAOi classes) of the wNAOi class (Figure 6c), while the intercept clearly decreases for smaller wNAOi classes (Figure 6b). Compared with the amount of precipitable water for the highest wNAOi class, the atmosphere contains only about 88.4 % for the lowest wNAOi class for the 6-month winter period for example. As a result, the precipitation history f becomes more sensitive to the rainout history

255 along the longitudinal gradient for lower wNAOi classes.

To summarise, the dependence of the *observed* longitudinal $\delta^{18}O_{pw}$ and δD_{pw} gradient on the class of wNAOi in the winter season results from two processes: (i) the changing continental temperature gradients via the temperature dependent isotope

fraction during condensation, which exerts the strongest influence on the $\delta^{18}O_{pw}$ and δD_{pw} gradient and (ii) the dependence of the amount of precipitable water or in general on the precipitation history, over central Europe on the wNAOi mode, which becomes important for more negative wNAOi classes. The latter mechanism is in agreement with recent findings of Aggarwal et al. (2012) who showed that, generally, more negative $\delta^{18}O_P$ values are associated with lower moisture residence times, where the moisture residence time is defined as the ratio between the amount of precipitable water and the precipitation (Aggarwal et al., 2012;Trenberth, 1998) and conclusions of (Rozanski et al., 1982) analysing summer and winter European δD_P longitudinal gradients

4.2 Alpine stations

By comparison with the low-altitude stations, the Alpine stations reveal more complex wNAOi - $\delta^{18}O_{pw}$, δD_{pw} patterns (Figure 3). North of the Alpine divide, all stations show similar $\delta^{18}O_{pw}$ and δD_{pw} - wNAOi class relationships as at the Garmisch-Partenkirchen GNIP station (Figure 2). The only exception to this relationship are the $\delta^{18}O_{pw}$ datasets for Thonon-Les-Bains, whose $\delta^{18}O_{pw}$ datasets have only a weak relationship to the wNAOi. The relationship between the $\delta^{18}O_{pw}$ - δD_{pw} values and wNAOi from stations at and south of the Alpine divide, including Grimsel (#18) (western Alps); Längenfeld (#21), Obergurgl (#23), Patscherkofel (#27) (all central Alps); Böckstein (#30), St. Peter (#31), Villacher Alpe (#32) and Graz (#33) (eastern Alps) is more complex compared to the stations north of the Alpine divide (see section 3.2 for detail).

The $\delta^{18}O_{pw}$, δD_{pw}, temperature and precipitation datasets were also grouped into six wNAOi classes according to respective wNAOi as previously for the non-Alpine stations (Section 4.1). A detailed analysis of the $\delta^{18}O_{pw}$ and δD_{pw} values of all Alpine stations shows that the median $\delta^{18}O_{pw}$ values become more negative for higher altitudes, irrespective of the wNAOi class. This observation is well known as the "altitude effect" (Dansgaard, 1954;Schürch et al., 2003). However, there is no obvious relationship ($p>0.1$ for all datasets) between the class of the wNAOi and the altitude effect for the Alpine stations (Fig. 7a and 7b). On average, the altitude effect is -0.32 ‰/100m (6-month average) and -0.30 ‰/100m (3-month average) for $\delta^{18}O_{pw}$ and -2.55 ‰/100m (6-months average) and -2.28 ‰/100m (3-months average) for δD_{pw} (Fig. 7a and 7b). Furthermore, the recorded air temperature at the Alpine stations change on average by about -0.58 and -0.56 K/100m for the 6-month and 3-month average, respectively, independent of the wNAOi class ($p>0.1$ for all datasets) (Fig. 7c). The mean values of the temperature-altitude relationship correspond approximately to the moist adiabatic lapse rate. Hence, a strong relationship between $\delta^{18}O_{pw}$ and δD_{pw} values and air temperature is observed in the Alpine stations (e.g. Schürch et al., 2003). No relationship between rainfall amount and $\delta^{18}O_{pw}$ was observed (Fig. 7d).

Because there is no relationship between the lapse rate and and/or precipitation amount with the wNAOi class, we conclude that the observed relationships between $\delta^{18}O_{pw}$ and δD_{pw} and the class of the wNAOi for our selection of Alpine stations are (i) caused by different air mass origins linked to wNAOi states and (ii) downstream effects of the varying central European continental effect that causes more negative $\delta^{18}O_{pw}$ and δD_{pw} values for more negative wNAOi classes. The weak or absent

relationships for stations at the Alpine divide can be caused by air masses of different origins (e.g. variable influences of the Mediterranean sourced moisture) (Kaiser et al., 2001). However, detailed back trajectories of rainfall events for the entire Alpine region would be required to further evaluate this explanation. Our analysis indicates that the Alpine divide exerts an

295   important influence on the winter hydrological cycle in the region, with precipitation north of the Alps sourced by atmospheric moisture originating from central Europe. In winter, this residual atmospheric moisture is already depleted in ^{18}O and ^{2}H when it reaches the northern part of the Alps, reflecting the ambient winter mode of the wNAOi, thereby determining the degree of the depletion in ^{18}O and ^{2}H in north Alpine winter precipitation.

To complete the above conclusion on the mixing of atmospheric moisture for stations at the Alpine divide, the

300    $\delta^{18}O_{pw}$ and δD_{pw} of circum-Mediterranean stations were also analysed for their dependence on the wNAOi (a discussion of the NAO-relationships between $\delta^{18}O_{pw}$ and δD_{pw} and temperature and precipitation can be found in the supplementary information). These stations are Avignon (34) (southwest of the Alps), Locarno (35) (south of Grimsel), Genoa (Setri) (south of the Alps) (36) and Zagreb (37) (southeast of the Alps) (Figure 1). For the 3-month $\delta^{18}O_{pw}$ and δD_{pw} data only those from Avignon and Zagreb shows a strong relationship to the wNAOi (about 1 ‰/wNAOi unit for $\delta^{18}O_{pw}$) (Figure 3a and 3c). For

305   the 6-month $\delta^{18}O_{pw}$ and δD_{pw} data, only the $\delta^{18}O_{pw}$ dataset from Locarno and the $\delta^{18}O_{pw}$ and δD_{pw} datasets from Zagreb show a relationship to wNAOi. The NAO-relationships of $\delta^{18}O_{pw}$ and δD_{pw} for the 3-month winter period from the Mediterranean stations Locarno and Genoa (Setri) show that the NAO-fingerprint, which is observed for Alpine stations north of the Alpine divide, is not transferred to these two stations. The situation might change for $\delta^{18}O_{pw}$ from Locarno for the 6-month winter period where a relationship to the wNAOi is observed. The stronger relationship for this winter period could be caused by an

310   increase of precipitation that results from air masses from central Europe. For Zagreb, it is difficult to explain the observed relationships between $\delta^{18}O_{pw}$ and δD_{pw}, because the closest Alpine stations show no relationship to the wNAOi. To further investigate the mechanisms that control the $\delta^{18}O_{pw}$ and δD_{pw} datasets in Avignon and Zagreb, the origin of the air masses in dependence on the wNAOi needs to be investigated further using isotope enabled regional climate models to better constrain the effect of local temperature and precipitation on $\delta^{18}O_{pw}$ and δD_{pw}. In summary, the variable wNAO-relationship of $\delta^{18}O_{pw}$

315   and δD_{pw} datasets from the investigated Mediterranean stations support the observation that the Alpine divide represents an important boundary region for the oxygen and hydrogen isotope system of Alpine precipitation.

5 Implications for palaeoclimate reconstructions from speleothems

5.1 Reconstructions from single speleothem-based carbonate $\delta^{18}O$

The results have important implications for palaeoclimate archives that record the $\delta^{18}O_{pw}$ and δD_{pw} values of winter

320   precipitation (October to March, the main period of infiltration in central Europe due to low evapo-transpiration rates). Potentially, such archives include speleothems and ground water. The following discussion focuses on speleothem carbonate $\delta^{18}O$ records, but is also applicable to speleothem fluid inclusion $\delta^{18}O$ and δD records, and is relevant for other palaeoclimate archives.

For a paleoclimate reconstruction that is based on a single speleothem from a cave site from central Europe or north
325 of the Alpine divide, $\delta^{18}O_{pw}$ and δD_{pw} values are typically lower for more negative wNAOi values (Figure 3). The median
sensitivity of $\delta^{18}O_{pw}$ from all continental stations is 0.57 ‰ per wNAOi unit. Hence, a persistent change of the average
wNAOi from e.g. +1 to -1 (i.e. -2 wNAOi units) would result in a reduction of the average $\delta^{18}O_{pw}$ by 1.14 ‰. Furthermore,
monthly average air temperatures are generally in phase with the wNAOi changes, resulting in a positive linear relationship
between $\delta^{18}O_{pw}$ and δD_{pw} and air temperatures. Hence, air temperatures tend to be lower depending on the cave location, if
330 the average wNAOi is smaller. This temperature-relationship was used recently to reconstruct historic $\delta^{18}O_{pw}$ values
(Mischel et al., 2015) and its use has been suggested for wNAOi reconstructions (Casado et al., 2013). Crucially, however,
the $\delta^{18}O_{pw}$ and δD_{pw} variability is controlled not only by changes in air temperature, but also by changes in the air mass
precipitation history (Section 4). Hence, the use of speleothem $\delta^{18}O$ values (or $\delta^{18}O$ and δD values from fluid inclusions or
ground water) to directly reconstruct the past variability of the wNAOi or winter temperatures should be undertaken
335 cautiously, because past changes of the hydrological cycle could result in a relationship between $\delta^{18}O_{pw}$ and temperature that
differs from the present day. This is particularly important for long-term reconstructions of atmospheric circulation. As for
the case of individual speleothem $\delta^{18}O$ records, caution should be exercised when interpreting changes in $\delta^{18}O$ gradients
inferred from multi-speleothem regression analysis because the continental precipitation $\delta^{18}O_{pw}$ and δD_{pw} gradients are
controlled by both the air temperature gradient and the air-mass precipitation history (Section 4).

340 Notwithstanding these caveats, the results from the sensitivity analysis of $\delta^{18}O_{pw}$ and air temperature theoretically
allow estimates of the possible influences of changes in $\delta^{18}O_{pw}$ and temperature for wNAOi changes on speleothem $\delta^{18}O$
records. For this exercise we use the station data of Stuttgart (Canstatt) (#8), located in southern Germany with a $\delta^{18}O_{pw}$ -
wNAOi sensitivity similar to the median of all continental stations. For the period from October to March, the NAO-
temperature relationship for this station suggests a sensitivity of 0.63 K/wNAOi unit, and an intercept of 4.38 °C (r=0.57); no
345 NAO-relationship is observed for precipitation amount. In the example above, a decrease in the NAO index from +1 to -1
would cause a change of -1.20 ‰ in $\delta^{18}O_{pw}$ in Stuttgart precipitation, with a concomitant decrease in air temperature of
approximately 1.26 K. Assuming that these changes in $\delta^{18}O_{pw}$ and air temperature on the surface are transmitted into a cave,
we can estimate both effects on speleothem $\delta^{18}O$ values. However, this is only reasonable for persistent changes of the NAO
on decadal to millennial time scales when there is sufficient time for thermal equilibration of the cave air temperature to
350 changes of the surface air temperature; and where any annual variability of the wNAO (i.e. 'noise') is overwhelmed by the
persistent change of the wNAO ('signal').

Applying the temperature sensitivity of the equilibrium oxygen-isotope fractionation factor of Kim and O'Neil
(1997) of about -0.22 ‰/K, the temperature change of -1.26 K would result in an increase in speleothem $\delta^{18}O$ by about
+0.28 ‰, but the simultaneous decrease by 1.20 ‰ in drip water $\delta^{18}O$ would dominate, resulting in an overall decrease in the
355 speleothem $\delta^{18}O$ by about 0.92 ‰. Therefore, the changes of precipitation $\delta^{18}O_{pw}$ would dominate the speleothem $\delta^{18}O$
record. We stress that these idealised conditions are rarely met in natural cave systems where other processes typically
influence the speleothem proxy values (e.g. isotope disequilibrium effects Deininger et al., 2012). Nonetheless, this exercise

emphasises that the sensitivity of $\delta^{18}O_{pw}$ to wNAOi is large and that persistent changes (i.e. centennial and millennial changes) in the mean state of the wNAO are likely to produce detectable and coherent changes in speleothem $\delta^{18}O$ time series in central Europe.

It is notable that for speleothems deposited in caves close to the Alpine divide where there is little or no relationship between $\delta^{18}O_{pw}$ and the wNAOi, speleothem $\delta^{18}O$ values are likely to be dominated by the temperature-dependent isotope fractionation factor during speleothem growth rather than by changes in $\delta^{18}O_{pw}$. Hence, if modern/historic temperature calibrations of speleothem $\delta^{18}O$ values are conducted, a relatively straightforward, but site-specific negative correlation between speleothem $\delta^{18}O$ and temperature is to be expected for sites close to the Alpine divide. This inference is supported by the two currently available studies; one at Spannagel Cave, Austria, which is located close to the Alpine divide in the central Alps where the temperature calibration is -0.44 ‰/K (Mangini et al., 2005) and one from Milandre Cave situated in the Swiss Jura Mountains (western Alps) approximately 150 km north of the Alpine divide, where the temperature calibration is 0.70 ‰/K (Fleitmann, 2016 personal communication). Taking the temperature sensitivity of $\delta^{18}O_{pw}$ of about 0.95 ‰/K for the GNIP station Konstanz, located at the similar latitude as Milandre Cave, and the temperature sensitivity of the equilibrium isotope fractionation between water and calcite of about -0.22‰/K, yields a net value of 0.73‰/K. This value is broadly consistent with the temperature calibration (0.70 ‰/K) found for Milandre Cave by Fleitmann.

The above discussion focused only on changes in $\delta^{18}O_{pw}$ and temperature that are transmitted into the cave. However, in natural cave systems, other environmental parameters linked to persistent changes of the wNAO could also influence speleothem $\delta^{18}O$. These include parameters such as cave air CO_2 concentrations (pCO$_2$), the Ca^{2+} concentration of drip waters or drip intervals. Modelling (e.g. Deininger et al., 2012;Mühlinghaus et al., 2009) and experimental work (e.g. Polag et al., 2010;Wiedner et al., 2008;Day and Henderson, 2011) reveal that these parameters can influence speleothem (calcite) $\delta^{18}O$ via isotope disequilibrium effects. These latter effects can in principle be as large as the NAO-related changes calculated above (see Deininger et al., 2012 for a thorough discussion on the sensitivity of all these parameters). Therefore, such reconstructions should be always undertaken cautiously , because they can include large uncertainties. Furthermore, $\delta^{18}O_{pw}$ variability can be smoothed during water percolation through the karst system, resulting in rather constant drip water $\delta^{18}O$ values which may further influence speleothem $\delta^{18}O$ (Mischel et al., 2015). The effects of these complications can be minimised through the use of well-monitored cave systems where the 'modern' (meaning over the duration of the monitoring period) cave system and the response of the diverse parameters monitored to natural changes of the surface conditions are well constrained, combined with appropriate forward models (e.g. ISOLUTION, Deininger et al., 2012) that allow estimates of the magnitude of these effect on speleothem $\delta^{18}O$. Further, the use of multiple coeval speleothem records from different cave systems can be regarded as a potential (new) approach to synthesise the common signal of all of these records (e.g. $\delta^{18}O$) using for example Principal Component Analysis (Deininger et al., 2016) or other statistical techniques (Rehfeld et al., 2013; Fischer, 2016).

5.2 Multiple speleothem-based reconstructions of Holocene longitudinal speleothem δ^{18}O gradients and implication on the evolution of the North Atlantic Oscillation

Although the aforementioned processes can modify speleothem δ^{18}O values, their effects might be negligible or at least less important when the palaeoclimate signals of multiple coeval speleothem δ^{18}O records are used to reconstruct past climate dynamics. As an example, McDermott et al. (2011) used δ^{18}O data for several coeval speleothems to show that longitudinal speleothem δ^{18}O gradients across Europe changed systematically during the Holocene. To compare the observed slopes and their temporal evolution during the Holocene and to evaluate a possible NAO-like mechanism the 6-month (October-March) longitudinal $\delta^{18}O_{pw}$ gradients need to be converted into expected speleothem (calcite) δ^{18}O gradients. Such estimates require that both the longitudinally variable winter temperature gradients (Figure 5a), as well as the $\delta^{18}O_{pw}$ slopes (Figure 4a) are taken into account. The effects of varying temperature gradients are considered via the temperature-dependent oxygen isotope fractionation between water and calcite. These estimates show that the slope of the longitudinal speleothem δ^{18}O gradient is expected to be greatest for the highest wNAOi class, decreasing for lower wNAOi classes. The calculated slopes for speleothem calcite based on the longitudinal $\delta^{18}O_{pw}$ slopes and air-temperature gradients of this study show remarkable agreement with a recent reconstruction of speleothem based δ^{18}O gradients throughout the Holocene (McDermott et al., 2011), (Figure 8).

Assuming that the present-day mechanisms that determine the observed relationships between the wNAOi and temperature, precipitation and $\delta^{18}O_{pw}$ are relevant for the boreal winter of the entire Holocene, the evolution of the reconstructed Holocene speleothem δ^{18}O gradients can be interpreted as reflecting changes in atmospheric pressure patterns akin to predominantly negative wNAOi-like modes in the early Holocene until about c. 8 ka, and mainly positive wNAOi-like modes during mid and late Holocene winters (this assumption includes caveats that are discussed further below). For this assumption (NAO type forcing), the changes of the speleothem δ^{18}O gradients are caused by changing temperature gradients (steeper west to east European temperature gradients in the early Holocene) and a changing precipitation history (increased precipitation and/or reduced amount of moisture in the atmosphere) linked to a NAO-like forcing. However, this interpretation requires that the NAO was operating akin to modern observations. In other words: it hypothesises that the Azores High and the Icelandic Low were broadly stationarity in space and time. A recent study has demonstrated recent (1871-2008 AD) non-stationarity of the Azores High (AH) and the Icelandic Low (IL), (expressed as the NAO angle index, which is positive when the IL is east of the AH and vice versa), but the latter is correlated with the wNAOi: a positive angle index tends to coincide with a positive wNAOi (Wang et al., 2012). For the Holocene, stationarity is hypothesised for the last 8 ka by Wassenburg et al. (2016) who proposed that the NAO reorganised between 9 ka and 8 ka ago in response to the melting Laurentide ice sheet and meltwater fluxes into the North Atlantic (Wassenburg et al., 2016). This study further suggests that the Icelandic Low was shifted southwest of its modern position during the early Holocene. The timing of this NAO reorganisation would be consistent with the finding of this study that the NAO switched from predominantly negative to positive wNAOi-like at about 8 ka. However, in contrast to the findings of Wassenburg et al., (2016), our study based on

the results of McDermott et al. (2011) would suggest a gradual shift of the IL and/or AH towards the northeast or southwest, respectively, during the course of the Holocene until stable boundary conditions are reached 5 to 4 ka ago.

The different inferences between this study (and that of McDermott et al., 2011) and Wassenburg et al. (2016) may be that the observations of Wassenburg et al. (2016) are based on two stalagmite proxy records only, located in North Germany and North Morocco whose proxy records are sensitive for the local amount of precipitation. The modern precipitation amount of the two regions is driven mainly by the NAO, but with opposite correlations, positive in North Germany and negative in North Morocco (cf. Figure 1b in Wassenburg et al., 2016). Hence, if these two speleothem precipitation-proxy records were compared from these two regions we would expect that, if the modern precipitation regimes had not changed, these two proxy records would be anti-correlated. If, however, the modern precipitation regimes changed (e.g. they shifted in response to changes of the atmospheric circulation) and if the local precipitation amount at the two locations change in the same direction, the two proxy records should be correlated. This scenario is exactly observed by Wassenburg et al. (2016) who show that the correlation between these two speleothem proxy records from North Germany and North Morocco changed from positive to negative between 9 ka and 8 ka (see Wassenburg et al., 2016 for details). However, the correlation of these two records is only a local perspective of the history on the amount of precipitation at these two individual locations and cannot resolve gradual changes of the precipitation pattern, but can only indicate whether the locations lie within the same hydrological regime or not. By contrast, the results of McDermott et al. (2011) that are further evaluated by this study are based on multiple speleothem $\delta^{18}O$ records that are distributed throughout Europe and are potentially more reliable to detect gradual changes. However, we emphasise that the results of our study and those of Wassenburg et al. (2016) do not contradict, but rather complement each other, and give two different views on the same phenomena, a gradual change of the 'NAO' during the Holocene that is likely caused by a relative shift of the IL and AH, mimicking NAO-like conditions in the speleothem $\delta^{18}O$ gradients. The synthesis of the aforementioned studies and the results presented here is that the relative location of the IL and AH changed gradually during the Holocene: in the early Holocene the IL and/or the AH were located southwest and northeast, respectively, of their modern positions, eventually mimicking negative NAO-like conditions and subsequently shifted northeastwards and southwestwards respectively during the Holocene, mimicking positive and modern NAO-like conditions, consistent with an independent study from the Iberian Peninsula (Walczak et al., 2015). This gradual change was potentially forced by the retreat of the Laurentide ice sheet during the early Holocene (Wassenburg et al., 2016) and possibly also by the changing Holocene wintertime insolation (McDermott et al., 2011;Walczak et al., 2015).

The approach applied by this study uses modern relationships between longitudinal precipitation $\delta^{18}O_{pw}$ gradients and the wNAOi and argues that the observed changes are caused i) by changing temperature gradients between west and east Europe and ii) a modified precipitation history f that accounts for changes in the amount of precipitable water in the atmosphere and in principle changing precipitation amounts. Though the latter (changes in the precipitation amount) was not evident in the analysed station datasets, there is no reason to exclude it for the Holocene interpretation of changing longitudinal speleothem

$\delta^{18}O$ gradients. This approach includes several caveats that need to be discussed in more detail. First, modern relationships are derived for yearly winter values (6 month and 3 month average values) that are derived mainly post 1961 AD (when the GNIP network begun). (The ECHAM5-wiso simulations used here also cover only the post 1960 AD period.) However in this period, the NAO angle index was rather stable and the relative location of the AH and IL did not vary much, compared to the period before (Wang et al., 2012). Hence, we cannot rule out any effect of the relative location of the AH and IL on the modern relationships between longitudinal $\delta^{18}O_{pw}$ gradients and the NAO and the conversion of the speleothem $\delta^{18}O$ gradients into wNAOi should be interpreted cautiously. Furthermore, recent studies have also highlighted that other atmospheric pressure systems (like the East Atlantic pattern) also exert an influence on European $\delta^{18}O_P$-NAO relationships (Comas-Bru et al., 2016), but did not study its relationship to the angle index of the NAO. This would be, however, interesting, because there might be relationships between the strength and location of the East Atlantic pattern and the angle index of the NAO (i.e. to the relative location between the AH and the IL). Second, a requirement for the interpretation of the changing longitudinal speleothem $\delta^{18}O$ gradients as variations of the NAO requires a time-stationary of the NAO back to the early Holocene. However, this requirement can be questioned based on the recent findings of Walczak et al. (2015) and Wassenburg et al. (2016) who demonstrated Holocene shifts of the AH and IL. Their conclusion is further supported by this study. Hence, the gradual shift of the speleothem $\delta^{18}O$ gradients during the Holocene should be interpreted as relative shifts of the AH and IL that are akin to the modes of the modern NAO (i.e. NAO-like) but likely have very different mechanism (ice sheets, insolation) forcing mechanisms on these longer timescales. Further research is necessary to illuminate these caveats extending on the one hand palaeoclimate investigations to generate new palaeoclimate proxy records and on the other hand conducting climate model simulations to study in detail the relationships between the dominating pressure systems and palaeoclimate proxy records as well as their underlying mechanism.

6 Conclusions and Summary

This study investigated the relationships between central European and Alpine $\delta^{18}O_{pw}$ and δD_{pw} values and the North Atlantic Oscillation index for the boreal winter (wNAOi). $\delta^{18}O_{pw}$ and δD_{pw} data for 37 meteorological stations distributed over central Europe and the Alps were analysed. This study demonstrates that the European continental isotope effect depends on the wNAOi, with steeper $\delta^{18}O_{pw}$ gradients associated with more negative wNAOi values. Hence, precipitation $\delta^{18}O_{pw}$ and δD_{pw} values across central Europe are more negative for lower wNAOi winters. We argue that the strength of this change is caused by (i) a steeper west to east continental air temperature gradient and (ii) a decrease in the precipitable water content of the atmosphere during more negative wNAOi conditions. (An evaluation of the longitudinal $\delta^{18}O_{pw}$ and δD_{pw} gradients from an isotope-enabled general circulation model, ECHAM5-wiso, shows that the simulated slopes are well reproduced compared with those reconstructed from observational data).

The emerging picture for Alpine stations is that for stations north of the alpine divide, $\delta^{18}O_{pw}$ and δD_{pw} values show a similar relationship to the wNAOi, as continental stations north of the Alps. However, in contrast with the processes that

determine $\delta^{18}O_{pw}$ and δD_{pw} values at continental stations, $\delta^{18}O_{pw}$ and δD_{pw} characteristics at Alpine stations are mainly a downstream residual effect of the changing continental effect. Furthermore, $\delta^{18}O_{pw}$ and δD_{pw} values of stations close to the Alpine divide in the central and eastern Alps exhibit a weak or absent relationship to the wNAOi. The results of this study have important implications for palaeoclimate reconstructions that are based on winter $\delta^{18}O_{pw}$ and δD_{pw} values, such as speleothem $\delta^{18}O$ records.

495

A simplistic interpretation of recent findings on the temporal evolution of longitudinal speleothem $\delta^{18}O$ gradients, assuming that modern NAO-related mechanisms are relevant for the Holocene, would be that the early Holocene was characterised by more negative NAO-like modes, while the mid and late Holocene would be characterised by more positive NAO-like modes. However, consistent with other independent studies (Wassenburg et al., 2016;Walczak et al., 2015) and an augmented NAO index that accounts for the relative position of the Azores High (AH) and Icelandic Low (IL) (Wang et al., 2012), we interpret the observed gradual Holocene change in longitudinal speleothem $\delta^{18}O$ gradients as a relative shift of the angular position of the AH and IL. These positions eventually evolve to situations akin to modern positive and negative NAO modes, but the millennial forcing mechanism during the course of the Holocene are likely to be different from the present day inter-annual to decadal variability. Further observational and modelling studies are necessary to better constrain the complex relationships between the atmospheric circulation and palaeoclimate proxy records.

500

505

Data availability

The processed data is available through supplementary material. Unprocessed data can be accessed through http://www-naweb.iaea.org/napc/ih/IHS_resources_gnip.html and https://wasser.umweltbundesamt.at/h2odb/.

Acknowledgement

510 We thank all operating organizations of the Global Network of Isotopes in Precipitation (GNIP) and the Austrian Network of Isotopes in Precipitation (ANIP) and all contributing researchers for their efforts to run and maintain the stations, which made this study possible. We are grateful to three anonymous reviewers for their constructive comments that help to improve the manuscript and to the associated editor Dominik Fleitmann for handling our manuscript. MD is funded by the Irish Research Council (IRC) by a Government of Ireland Postdoctoral Fellowship (GOIPD/2015/789). FMcD acknowledges

515 support from Science Foundation Ireland through its Research Frontiers Program (RFP) Grants 07/RFP/GEOF265 and 08/FRP/GEO1184.

References

Aggarwal, P. K., Alduchov, O. A., Froehlich, K. O., Araguas-Araguas, L. J., Sturchio, N. C., and Kurita, N.: Stable isotopes in global precipitation: A unified interpretation based on atmospheric moisture residence time, Geophysical Research Letters, 39, 2012.

Baldini, L. M., McDermott, F., Foley, A. M., and Baldini, J. U. L.: Spatial variability in the European winter precipitation δ18O-NAO relationship: Implications for reconstructing NAO-mode climate variability in the Holocene, Geophysical Research Letters, 35, L04709-L04709, 2008.

Barnston, A. G., and Livezey, R. E.: Classification, seasonality and persistence of low-frequency atmospheric circulation patterns, Monthly weather review, 115, 1083-1126, 1987.

Casado, M., Ortega, P., Masson-Delmotte, V., Risi, C., Swingedouw, D., Daux, V., Genty, D., Maignan, F., Solomina, O., and Vinther, B.: Impact of precipitation intermittency on NAO-temperature signals in proxy records, Climate of the Past, 9, 871-886, 2013.

Comas-Bru, L., and McDermott, F.: Impacts of the EA and SCA patterns on the European twentieth century NAO-winter climate relationship, Quarterly Journal of the Royal Meteorological Society, 2013.

Comas-Bru, L., McDermott, F., and Werner, M.: The effect of the East Atlantic pattern on the precipitation δ18O-NAO relationship in Europe, Climate Dynamics, 47, 2059–2069, 2016.

Craig, H.: Isotopic variations in meteoric waters, Science, 133, 1702-1703, 1961.

Craig, H., and Gordon, L. I.: Deuterium and oxygen 18 variations in the ocean and the marine atmosphere, Consiglio nazionale delle richerche, Laboratorio de geologia nucleare, 1965.

Dansgaard, W.: The O 18-abundance in fresh water, Geochimica et Cosmochimica Acta, 6, 241-260, 1954.

Dansgaard, W.: Stable isotopes in precipitation, Tellus, 16, 436-468, 1964.

Day, C. C., and Henderson, G. M.: Oxygen isotopes in calcite grown under cave-analogue conditions, Geochimica et Cosmochimica Acta, 75, 3956-3972, 2011.

Deininger, M., Fohlmeister, J., Scholz, D., and Mangini, A.: Isotope disequilibrium effects: The influence of evaporation and ventilation effects on the carbon and oxygen isotope composition of speleothems-A model approach, Geochimica et Cosmochimica Acta, 2012.

Deininger, M., McDermott, F., Mudelsee, M., Werner, M., Frank, N., and Mangini, A.: Coherency of late Holocene European speleothem δ18O records linked to North Atlantic Ocean circulation, Climate Dynamics, 2016.

Eriksson, E.: Deuterium and oxygen-18 in precipitation and other natural waters Some theoretical considerations, Tellus A, 17, 1965.

Field, R. D.: Observed and modeled controls on precipitation δ18O over Europe: From local temperature to the Northern Annular Mode, Journal of Geophysical Research: Atmospheres (1984–2012), 115, 2010.

Fischer, M. J., and Baldini, L. M.: A climate-isotope regression model with seasonally-varying and time-integrated relationships, Climate dynamics, 37, 2235-2251, 2011.

Fischer, M. J.: Predictable components in global speleothem δ 18 O, Quaternary Science Reviews, 131, 380-392, 2016.

Gat, J. R.: Oxygen and hydrogen isotopes in the hydrologic cycle, Annual Review of Earth and Planetary Sciences, 24, 225-262, 1996.

Gulev, S. K., Zolina, O., and Grigoriev, S.: Extratropical cyclone variability in the Northern Hemisphere winter from the NCEP/NCAR reanalysis data, Climate Dynamics, 17, 795-809, 2001.

Humer, G.: NIEDERSCHLAGSISOTOPENNETZ ÖSTERREICH. Daten, 1995.

Hurrell, J. W.: Decadal Trends in the North-Atlantic Oscillation - Regional Temperatures and Precipitation, Science, 269, 676-679, 1995.

Hurrell, J. W., and VanLoon, H.: Decadal variations in climate associated with the north Atlantic oscillation, Climatic Change, 36, 301-326, 1997.

Hurrell, J. W., Kushnir, Y., Ottersen, G., and Visbeck, M.: The North Atlantic Oscillation: climatic significance and environmental impact, American Geophysical Union, 2003.

Kaiser, A., Scheifinger, H., Kralik, M., Papesch, W., Rank, D., and Stichler, W.: Links between meteorological conditions and spatial/temporal variations in long-term isotope records from the Austrian precipitation network, C&SPaperSeries, 13, 67-77, 2001.

Kim, S.-T., and O'Neil, J. R.: Equilibrium and nonequilibrium oxygen isotope effects in synthetic carbonates, Geochimica et Cosmochimica Acta, 61, 3461-3475, 1997.

Langebroek, P. M., Werner, M., and Lohmann, G.: Climate information imprinted in oxygen-isotopic composition of precipitation in Europe, Earth and Planetary Science Letters, 2011.

570   Lykoudis, S. P., and Argiriou, A. A.: Temporal trends in the stable isotope composition of precipitation: a comparison between the eastern Mediterranean and central Europe, Theoretical and applied climatology, 105, 199-207, 2011.

Mangini, A., Spötl, C., and Verdes, P.: Reconstruction of temperature in the Central Alps during the past 2000 yr from a δ 18 O stalagmite record, Earth and Planetary Science Letters, 235, 741-751, 2005.

McDermott, F., Atkinson, T. C., Fairchild, I. J., Baldini, L. M., and Mattey, D. P.: A first evaluation of the spatial gradients 575   in δ18O recorded by European Holocene speleothems, Global and Planetary Change, 79, 275-287, 2011.

Mischel, S. A., Scholz, D., and Spötl, C.: δ18O values of cave drip water: a promising proxy for the reconstruction of the North Atlantic Oscillation?, Climate Dynamics, 1-16, 2015.

Mook, W. G.: Introduction to isotope hydrology, Taylor & Francio, 8, 2006.

Mühlinghaus, C., Scholz, D., and Mangini, A.: Modelling fractionation of stable isotopes in stalagmites, Geochimica et 580   Cosmochimica Acta, 73, 7275-7289, 2009.

Polag, D., Scholz, D., Mühlinghaus, C., Spötl, C., Schröder-Ritzrau, A., Segl, M., and Mangini, A.: Stable isotope fractionation in speleothems: Laboratory experiments, Chemical Geology, 279, 31-39, 2010.

Rayleigh, L.: LIX. On the distillation of binary mixtures, The London, Edinburgh, and Dublin Philosophical Magazine and Journal of Science, 4, 521-537, 1902.

585   Rehfeld, K., Marwan, N., Breitenbach, S. F. M., and Kurths, J.: Late Holocene Asian summer monsoon dynamics from small but complex networks of paleoclimate data, Climate dynamics, 41, 3-19, 2013.

Rozanski, K., Sonntag, C., and Münnich, K. O.: Factors controlling stable isotope composition of European precipitation, Tellus, 34, 142-150, 1982.

Rozanski, K., Araguás-Araguás, L., and Gonfiantini, R.: Relation between long-term trends of oxygen-18 isotope 590   composition of precipitation and climate, Science, 258, 981-985, 1992.

Schürch, M., Kozel, R., Schotterer, U., and Tripet, J.-P.: Observation of isotopes in the water cycle—the Swiss National Network (NISOT), Environmental Geology, 45, 1-11, 2003.

Stumpp, C., Klaus, J., and Stichler, W.: Analysis of long-term stable isotopic composition in German precipitation, Journal of Hydrology, 517, 351-361, 2014.

595   Trenberth, K. E.: Atmospheric moisture residence times and cycling: Implications for rainfall rates and climate change, Climatic change, 39, 667-694, 1998.

Trigo, R. M., Osborn, T. J., and Corte-Real, J. M.: The North Atlantic Oscillation influence on Europe: climate impacts and associated physical mechanisms, Climate Research, 20, 9-17, 2002.

Walczak, I. W., Baldini, J. U. L., Baldini, L. M., McDermott, F., Marsden, S., Standish, C. D., Richards, D. A., Andreo, B., 600   and Slater, J.: Reconstructing high-resolution climate using CT scanning of unsectioned stalagmites: A case study identifying the mid-Holocene onset of the Mediterranean climate in southern Iberia, Quaternary Science Reviews, 127, 117-128, 2015.

Wang, Y. H., Magnusdottir, G., Stern, H., Tian, X., and Yu, Y.: Decadal variability of the NAO: introducing an augmented NAO index, Geophysical Research Letters, 39, 2012.

605   Wassenburg, J. A., Dietrich, S., Fietzke, J., Fohlmeister, J., Jochum, K. P., Scholz, D., Richter, D. K., Sabaoui, A., Spötl, C., Lohmann, G., Andreae, M. O., and Immenhauser, A.: Reorganization of the North Atlantic Oscillation during early Holocene deglaciation, Nature Geoscience, 2016.

Werner, M., Langebroek, P. M., Carlsen, T., Herold, M., and Lohmann, G.: Stable water isotopes in the ECHAM5 general circulation model: Toward high-resolution isotope modeling on a global scale, Journal of Geophysical Research, 116, 610   D15109-D15109, 2011.

Wiedner, E., Scholz, D., Mangini, A., Polag, D., Mühlinghaus, C., and Segl, M.: Investigation of the stable isotope fractionation in speleothems with laboratory experiments, Quaternary International, 187, 15-24, 2008.

Tables

	W-E difference for $\delta^{18}O_{pw}$								W-E difference for δD_{pw}							
	Observed		Calculated		Deviation				Observed		Calculated		Deviation			
wNAOi class	6m	3m	6m	3m	6m		3m		6m	3m	6m	3m	6m		3m	
	‰	‰	‰	‰	‰	%	‰	%	‰	‰	‰	‰	‰	%	‰	%
I: 1.77	4.78	6.02	3.75	4.98	**1.03**	*22.5*	**1.04**	*17.3*	42.62	52.10	32.80	43.56	**9.82**	*23.0*	**8.54**	*16.4*
II: 1.18	4.94	5.14	3.28	3.98	**1.66**	*33.6*	**1.16**	*22.6*	44.06	46.19	28.72	34.84	**15.34**	*34.8*	**11.35**	*25.8*
III: 0.40	5.73	6.32	4.00	5.54	**1.73**	*30.2*	**0.79**	*12.5*	49.37	51.68	35.01	48.44	**14.36**	*29.1*	**3.24**	*6.3*
IV: -0.46	6.66	7.89	4.18	5.58	**2.48**	*37.2*	**2.31**	*29.3*	56.93	65.10	36.58	48.81	**20.35**	*35.7*	**16.29**	*25.0*
V: -1.17	6.22	7.38	4.44	6.55	**1.79**	*28.8*	**0.83**	*11.2*	53.44	61.11	38.82	57.31	**14.62**	*27.4*	**3.80**	*6.2*
VI: -2.23	6.54	7.56	3.37	5.05	**3.17**	*48.5*	**2.51**	*33.2*	54.61	64.56	29.46	44.21	**25.14**	*46.0*	**20.35**	*31.5*

Table 1. Differences in $\delta^{18}O_{pw}$ and δD_{pw} (6 month (6m) and 3 month (3m) winter periods) between the western- (Valentia, Ireland) and eastern-most station (Krakow, Poland) for all wNAOi classes based on continental GNIP station datasets. The median wNAOi for classes I to VI respectively are: 1.77, 1.18, 0.40, -0.46, -1.17 and -2.23. The empirical estimates for the *observed* W-E difference of $\delta^{18}O_{pw}$ and δD_{pw} presented here are based on linear regressions of the observed trends (Figure 4). The *calculated* $\delta^{18}O_{pw}$ and δD_{pw} values are based on the temperature difference between Valentia (Ireland) and Krakow (Poland) estimated from the linear regression of the continental GNIP station temperature datasets and temperature sensitivities for $\delta^{18}O_P$ and δD_P from Dansgaard (1964). Deviation (bold numbers) means the difference between observed and calculated $\delta^{18}O_{pw}$ and δD_{pw} values. The italic numbers states the deviation relative to the observed difference given in %.
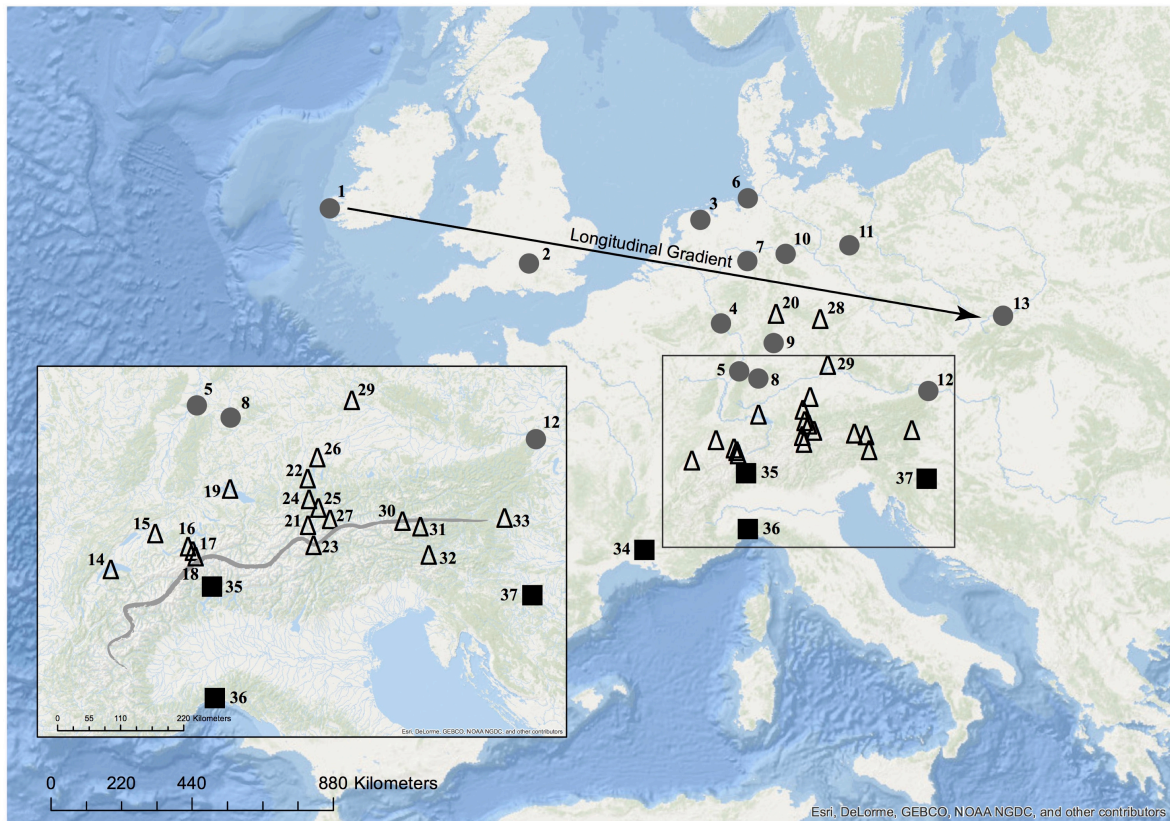
Figures

Figure 1. Map showing the location of all investigated stations: closed grey circles show the location of continental stations (altitude ≤350m with no Mediterranean influence); open triangles indicate alpine and high altitude (>350m) stations; closed squares show the location of 'Mediterranean influenced' stations. The grey line in the box indicates the Alpine Divide. Station codes for continental stations (from west to east): 1) Valentia (Observatory); 2) Wallingford; 3) Groningen; 4) Koblenz; 5) Karsruhe; 6) Cuxhaven; 7) Bad Salzulfen; 8) Stuttgart (Cannstatt); 9) Würzburg; 10) Braunschweig; 11) Berlin; 12) Vienna (Hohe Warte); 13) Krakow (Wola Justowska). For high altitude stations: 14) Thonon-Les-Bains; 15) Bern; 16) Meiringen; 17) Guttannen; 18) Grimsel; 19) Konstanz; 20) Wasserkuppe-Rhoen; 21) Längenfeld; 22) Hohenpeisenberg; 23) Obergurgl; 24) Garmisch-Partenkirchen; 25) Scharnitz; 26) Neuherberg; 27) Patscherkofel; 28) Hof-Hohensaas; 29)

Regensburg; 30) Böckstein; 31) St. Peter; 32) Villacher Alpe; 33) Graz Universität. For Mediterranean influenced stations: 34) Avignon; 35) Locarno; 36) Genoa (Sestri); 37) Zagreb.

660
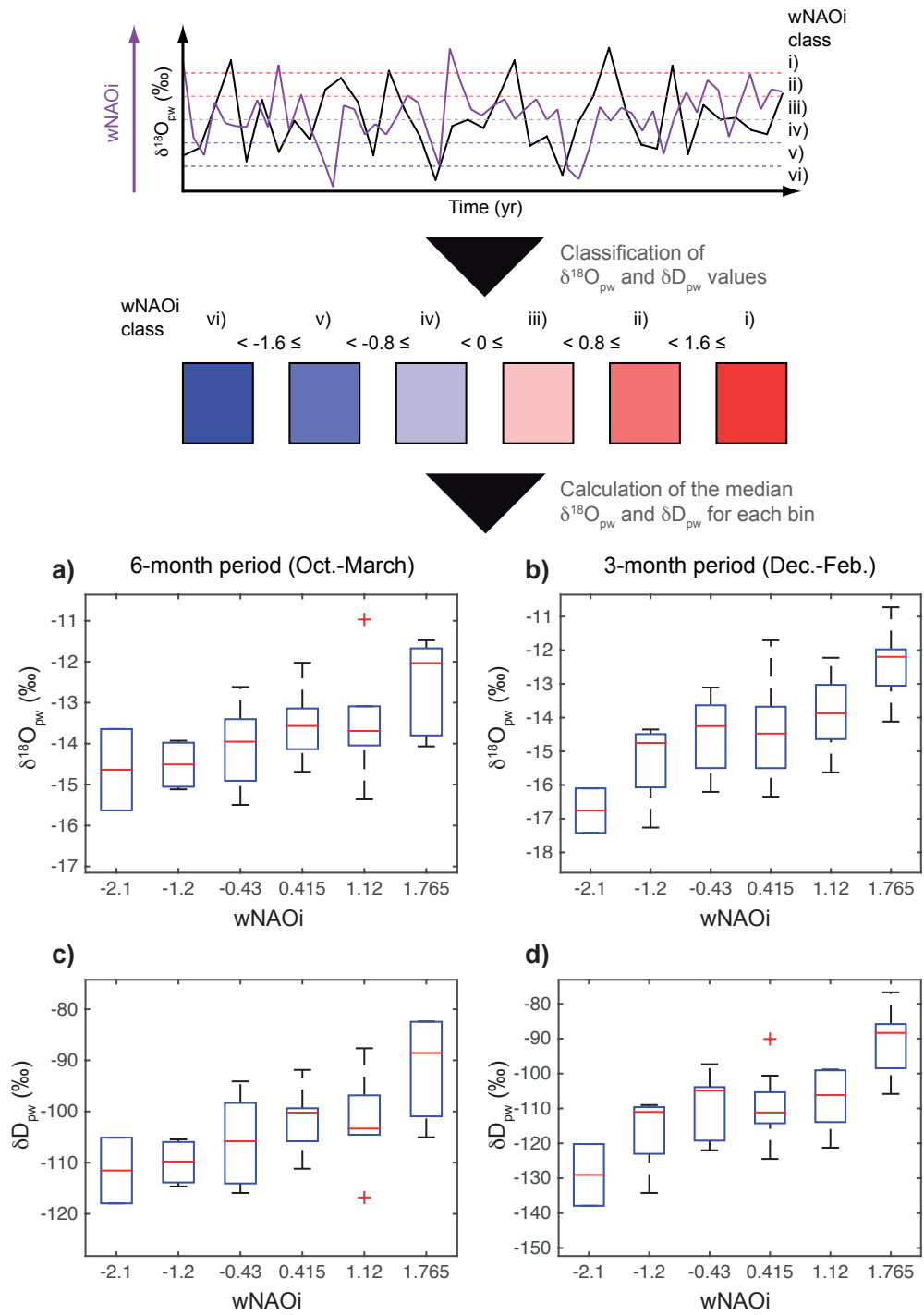
Figure 2. The upper part of the figure depicts how the precipitation weighted $\delta^{18}O_{pw}$ and δD_{pw} values are classified here into six classes depending on the wNAOi. Median values are calculated for every class, and this is used for further analysis. Panel a) to d) show the processed results for the six classes for one exemplar GNIP station (Garmisch-Partenkirchen, Germany), for which $\delta^{18}O_{pw}$ and δD_{pw} values have a typical sensitivity to wNAOi (see Figure 3). The left panels show the box plots for the 6 months period (October to March) and the right panels for the 3 months period (December to February). The upper panels illustrate the $\delta^{18}O_{pw}$ values, the lower panels the δD_{pw} values. Every box plot illustrates the statistical variables (median, min, max, 25 and 75% quantile) for every wNAOi class from lowest to highest (left to right). For the individual wNAOi classes, the red line illustrates the median of the data compilation; the edges of the blue rectangles mark the 25% and 75% quantile; the black bars illustrates the minimum and maximum values and the red cross denotes 'outliers'.
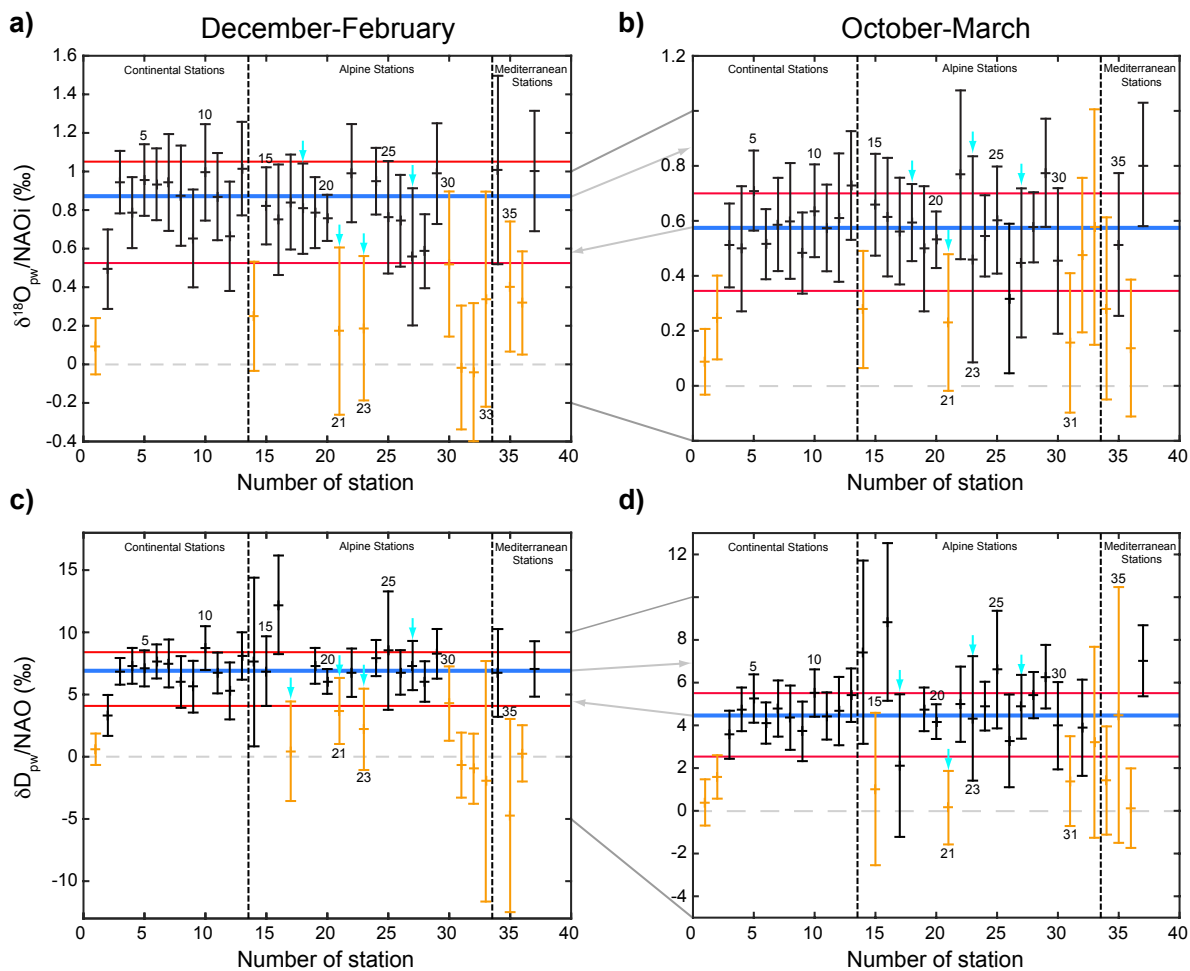
Figure 3. The panels illustrate the slopes of the linear regressions between yearly $\delta^{18}O_{pw}$ (a and b) and δD_{pw} (c and d) and the wNAOi for each individual station for the 3-month winter period (December-February) (left panels) and the 6-month winter period (October-March) (right panels). If the slope is illustrated in black the linear correlation coefficient is greater than 0.3; otherwise it is shown in orange. The blue lines indicate the median values of all continental stations; the upper and lower red lines highlight the 1-sigma standard deviation around the mean value. The grey dashed lines indicate a slope of 0 (i.e. no sensitivity). Station Garmisch-Partenkirchen (24) whose sensitivity on the wNAOi classes is shown in detail in Figure 2 is typical of the investigated stations. The cyan coloured arrows indicate stations closest to the Alpine Divide. Numbers indicate station codes as in Figure 1.
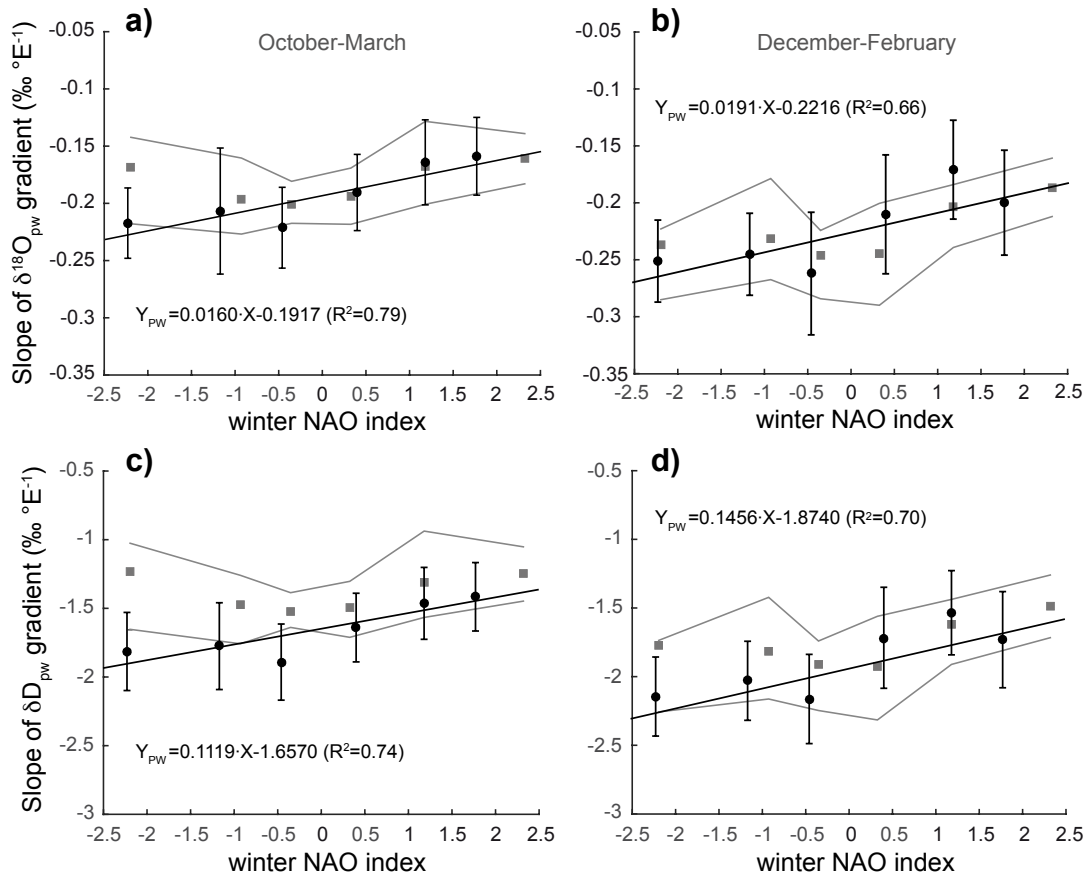
690

Figure 4: Illustration of the slopes of the $\delta^{18}O_{pw}$ (a and b) and δD_{pw} (c and d) longitudinal gradients across Europe (filled circles) – and their respective standard errors – calculated from 13 continental GNIP stations for the 6-month (October-March) (a and c) and 3-month (December to February) (b and d) winter period. More negative wNAOi classes result in a steeper isotope gradient across Europe in winter and, therefore, more strongly depleted $\delta^{18}O_{pw}$ and δD_{pw} values with

695   increasing distance (towards the east) from the European western margin. The coefficient for the linear regression between the observed slopes and the class of the wNAOi is 0.016±0.004 (r^2=0.79; p<0.05) for Fig. 1a, 0.019±0.006 (r^2=0.65; p=0.0502) for Fig. 1b; 0.111±0.033 (r^2=0.74, p<0.05) for Fig. 1c and 0.146±0.048 (r^2=0.70, p<0.05) for Fig 1d (units are ‰ °E^{-1}/wNAOi). These equations state the results from the linear regression where Y_{PW} is the slope of the $\delta^{18}O_{pw}$ or δD_{pw} gradient and X is the wNAOi. The filled grey squares show the median slopes of the ECHAM5-wiso simulations; the grey

700   envelope indicates the 25% and 75% quantiles of the ECHAM5-wiso slopes.
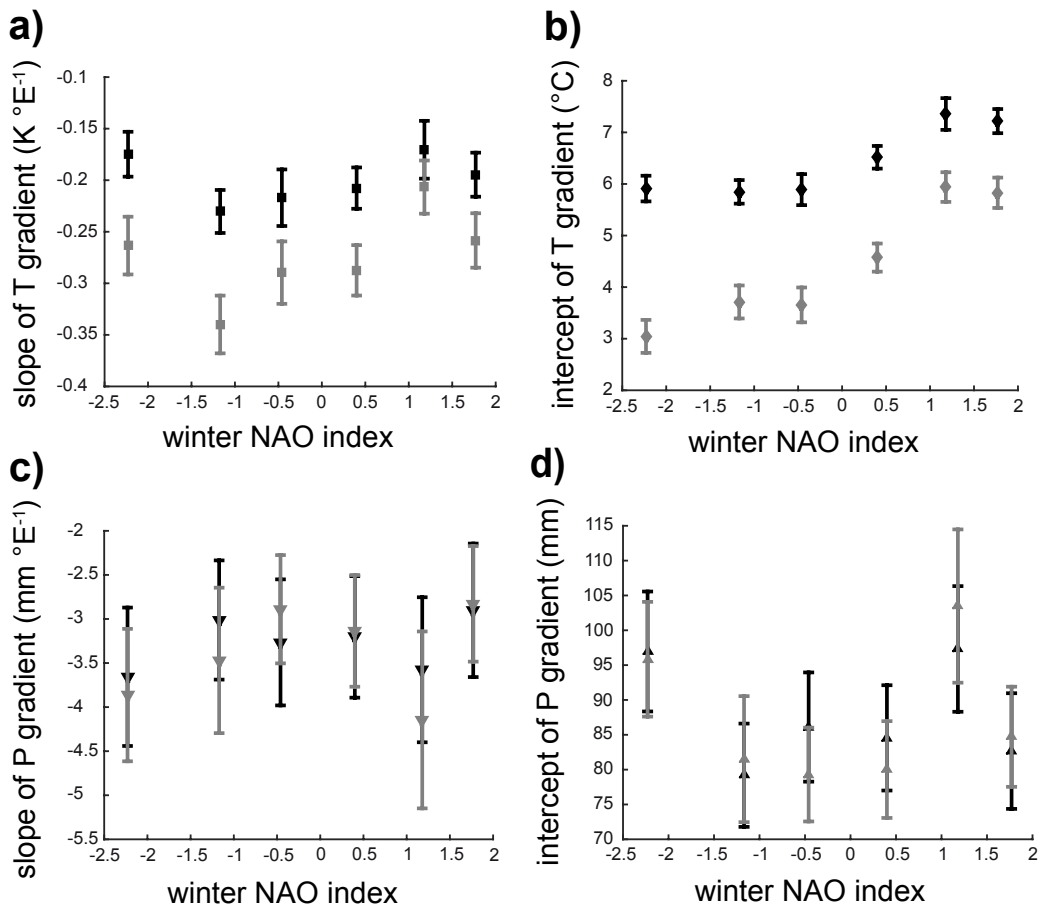
705 **Figure 5.** Based on observational data only, these four panels illustrate the slope of the continental gradient for (a) temperature and (c) precipitation as a function of the class of wNAOi that are calculated from GNIP station datasets. Panel b) and d) shows the intercepts of the linear regression for the continental temperature and precipitation gradients versus the wNAOi, respectively. Black symbols indicate the results for the 6-month winter period (October-March); grey symbols denote results for the 3-month (December-February) winter period. The slopes for temperature and precipitation show no

710 relationship to the wNAOi if all six classes are analysed (p>0.1). However, omitting the most negative wNAOi class yields a significant linear correlation of 0.71 and 0.67 (p<0.01) for the 6 and 3 month averages, respectively. While there is no significant relationship between the intercept of the precipitation gradients with the wNAOi (p>0.1), the intercept of the air temperature gradients shows a clear trend, with lower temperatures associated with lower wNAOi values.

715
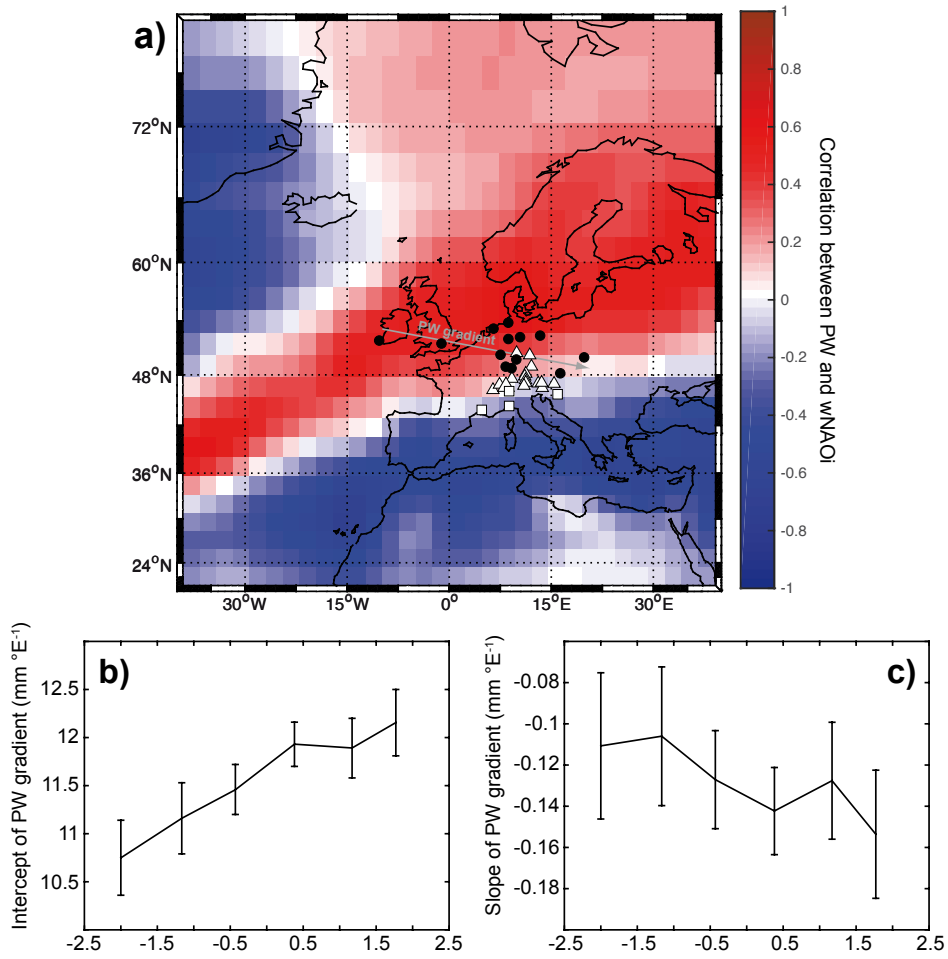
Figure 6: a) Correlation map between the wNAOi and the amount of precipitable water (PW) for the month December to March based on NCEP/NCER reanalysis data for the period 1948-2016 and the results of the longitudinal gradient (b) intercept; c) slope) for grid cells where continental stations are located (closed circles). Open triangles show the location of Alpine stations; open squares indicate the position of Mediterranean influenced stations.
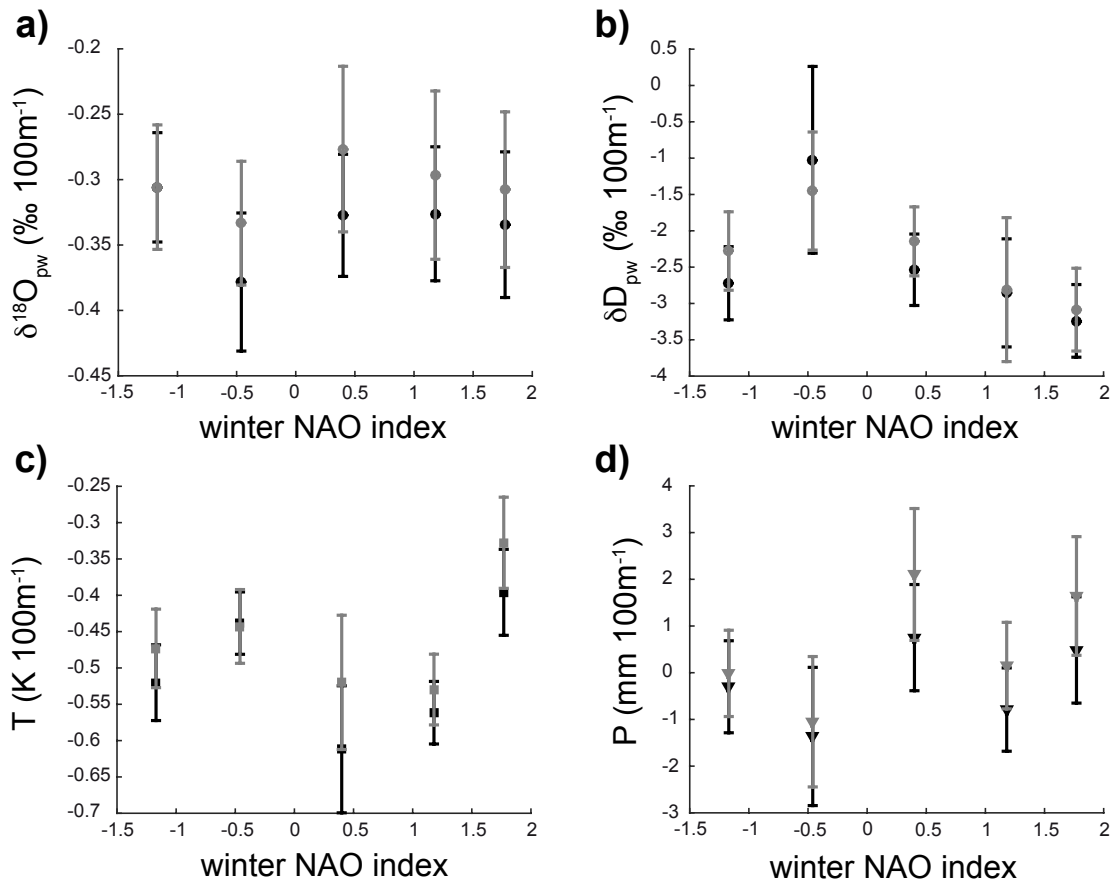
Figure 7: The four panels show the rate of change of (a) $\delta^{18}O_{pw,}$ (b) δD_{pw}, (c) temperature (T) and (d) precipitation (P) as a function of altitude for different wNAOi classes. (The lowest wNAOi class was not analysed because data of only four stations (out of 17) is available.) All Alpine stations are included. None of the correlations are statistically significant (p>0.1). Black symbols indicate the results of the 6-month winter period; grey symbols denote the 3-month winter period.
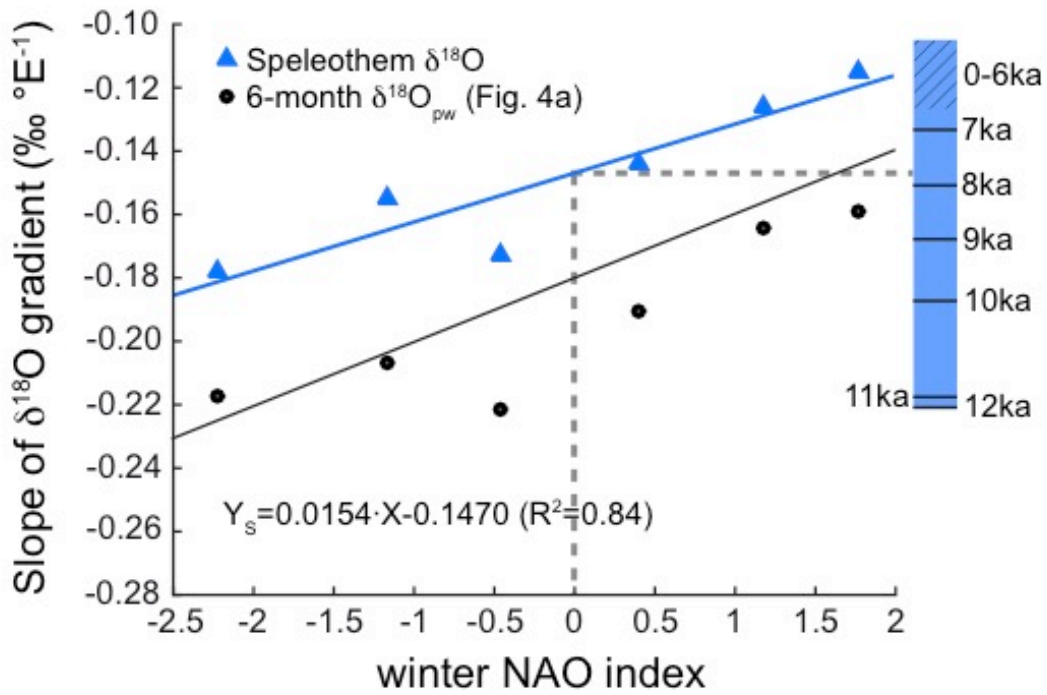
Figure 8: The blue triangles illustrate the forward-modelled longitudinal slopes for speleothem records calculated for each wNAOi class from their respective 6-months (October-March) longitudinal $\delta^{18}O_{pw}$ gradients (closed circles) and the observed temperature gradient converted into a speleothem $\delta^{18}O$ gradient using a sensitivity of 0.225 ‰/K (Kim and O'Neil, 1997). The blue and black line indicates the regression line from the longitudinal speleothem $\delta^{18}O$ and $\delta^{18}O_{pw}$ gradient, respectively. The blue bar highlights the range of reconstructed longitudinal speleothem $\delta^{18}O$ slopes during the Holocene (McDermott et al., 2011). The temporal evolution of the speleothem $\delta^{18}O$ slopes (McDermott et al. (2011) vary between -0.2208 ‰/°E and -0.1336 ‰/°E from 12 ka to 7 ka, and vary and between -0.1266 ‰/°E and -0.1046 ‰/°E from 6 ka to the present (shaded area). Comparison of the speleothem slopes with those calculated in this study suggests predominantly wNAO- like-modes in the early Holocene until about c. 8 ka and wNAO+ like-modes in the mid and late Holocene.